



Published in final edited form as:

Cancer Cytopathol. 2018 December ; 126(12): 992–1002. doi:10.1002/cncy.22071.

Clues to Recognition of Fumarate Hydratase-Deficient Renal Cell Carcinoma: Findings From Cytologic and Limited Biopsy Samples

Irene Shyu, MD¹, Leili Mirsadraei, MD², Xiaoyan Wang, MD, PhD³, Valentina Robila, MD, PhD¹, Rohit Mehra, MD⁴, Jonathan B. McHugh, MD⁴, Ying-Bei Chen, MD, PhD², Aaron M. Udager, MD, PhD⁴, Anthony J. Gill, MD⁵, Liang Cheng, MD³, Mahul B. Amin, MD⁶, Oscar Lin, MD, PhD², Steven Christopher Smith, MD, PhD^{1,7}

¹Department of Pathology, Virginia Commonwealth University (VCU) School of Medicine, Richmond, Virginia

²Department of Pathology, Memorial Sloan Kettering Cancer Center, New York, New York

³Department of Pathology and Laboratory Medicine, Indiana University School of Medicine, Indianapolis, Indiana

⁴Department of Pathology, Michigan Medicine, Ann Arbor, Michigan

⁵Cancer Diagnosis and Pathology Group, Kolling Institute of Medical Research, Royal North Shore Hospital and University of Sydney, Sydney, New South Wales Australia

⁶Department of Pathology and Laboratory Medicine, University of Tennessee Health Sciences, Memphis, Tennessee

⁷Department of Surgery, VCU School of Medicine, Richmond, Virginia

Abstract

BACKGROUND: Fumarate hydratase (FH)-deficient renal cell carcinoma (RCC) is rare and highly aggressive and is believed to arise mostly in the setting of hereditary leiomyomatosis-RCC syndrome with a germline mutation of FH. Because of the aggressiveness of these tumors and a frequent lack of ascertainable family history, these tumors may first present as metastases and

Corresponding author: Steven Christopher Smith, MD, PhD, Department of Pathology, Virginia Commonwealth University School of Medicine, 1200 E Marshall Street; Richmond, VA 23298; steven.c.smith@vcuhealth.org.

AUTHOR CONTRIBUTIONS

Irene Shyu: Data curation, formal analysis, investigation, and writing—original draft. **Leili Mirsadraei:** Data curation, formal analysis, investigation, and writing—review and editing. **Xiaoyan Wang:** Investigation, data curation, and writing—review and editing. **Valentina Robila:** Formal analysis and writing—original draft. **Rohit Mehra:** Investigation and writing—review and editing. **Jonathan B. McHugh:** Investigation and writing—review and editing. **Ying-Bei Chen:** Data curation, formal analysis, investigation, and writing—review and editing. **Aaron M. Udager:** Data curation, investigation, and writing—review and editing. **Anthony J. Gill:** Data curation, investigation, and writing—review and editing. **Liang Cheng:** Data curation, investigation, and writing—review and editing. **Mahul B. Amin:** Conceptualization and writing—review and editing. **Oscar Lin:** Conceptualization, investigation, formal analysis, and writing—review and editing. **Steven Christopher Smith:** Conceptualization, investigation, formal analysis, and writing—original draft.

CONFLICT OF INTEREST DISCLOSURES

Steven Christopher Smith reports royalties for textbooks from Elsevier/Amirsys Publishing outside the submitted work. The remaining authors made no disclosures.

be sampled by cytology. The cytologic findings of FH-deficient RCC have not previously been reported.

METHODS: Cytologic and limited biopsy samples from patients with FH-deficient RCC were reviewed retrospectively.

RESULTS: In total, 24 cytologic and limited biopsy samples from 19 patients (6 women and 13 men; age range, 22–69 years) who had FH-deficient RCC and metastasis at presentation were evaluated. These included 21 cytology samples ranging from malignant effusions (n = 7) to metastases (n = 11), to samples of primary kidney tumors (n = 3). The samples exhibited cells, often in clusters and abortive papillae, with voluminous, finely vacuolated cytoplasm and large, pleomorphic nuclei with prominent, viral inclusion-like nucleoli. A distinctive finding of peripheral cytoplasmic clearing frequently was apparent, and intranuclear cytoplasmic pseudoinclusions were less frequent. Of 7 cell block and biopsy samples, several of which represented sampling from the same patient, all demonstrated tissue fragments that had discernable morphologic patterns associated with FH-deficient RCC, including tubulocystic and intracystic papillary growth.

CONCLUSIONS: Features characteristic and suggestive of FH-deficient RCC may be identified in cytologic and small biopsy samples. Although the current samples were identified retrospectively in well characterized cases of FH-deficient RCC, the authors argue that, with appropriate clinical correlation, these features are sufficiently distinctive to trigger recognition and confirmatory workup.

Keywords

aspiration cytology; fumarate hydratase-deficient renal cell carcinoma; hereditary leiomyomatosis-renal cell carcinoma syndrome; hereditary neoplasia; renal cell carcinoma

INTRODUCTION

Hereditary leiomyomatosis-renal cell carcinoma (HLRCC) syndrome is an autosomal dominantly inherited, neoplastic diathesis characterized by a penetrant (approximately 80%) phenotype of uterocutaneous leiomyomatosis, with a less penetrant phenotype (approximately 5%–20%; varies according to the cohort studied) of high-grade renal cell carcinoma (RCC).¹ Affected individuals harbor germline mutations or deletions of the fumarate hydratase (*FH*) gene located on chromosome 1q42.3-q43.² The RCCs arising in this syndrome exhibit variable morphology with a high multiplicity of patterns³ and arise across a wide age range. However, in contradistinction to several other hereditary RCC syndromes, with few exceptions,^{4,5} these tumors tend to have highgrade morphology and an aggressive clinical course.⁶

Despite the wide variation in architectural patterns described in these RCCs, including papillary, tubulopapillary, solid, cribriform, and cystic patterns, sections of these tumors tend to exhibit a striking, viral inclusion-like, orangeophilic macronucleolus with a perinucleolar halo of clearing.⁶ Now an accepted entity in the World Health Organization classification,⁷ increasing scholarship has confirmed the broad morphologic range^{8,9} and relatively frequent

tubulocystic pattern,¹⁰ which appears to be a useful morphologic marker for differentiation from other high-grade, infiltrative renal tumors.¹¹

Most relevant to prospective diagnostic practice, recent reports have established the utility of immunohistochemistry for FH^{8,12} and antibodies detecting aberrant succination (anti-S-[2-succino]-cysteine [2SC])⁹ for the recognition of these tumors. On the basis of experience with FH and 2SC in the workup of kidney tumors, noting many cases with immunohistochemical and morphologic findings suggestive of HLRCC syndrome but nearly always without available data on stigmata, family history, or genetic testing at the time of sign out, we recently proposed the term *FH-deficient RCC* as a provisional diagnostic term¹⁰ to phenotypically label cases. This term avoids appearing to diagnose a genetic syndrome without appropriate workup and is amenable to (likely rare) sporadic, nonsyndromic cases of FH-deficient RCC occurring by somatic mutation only.^{10,13} The term is to be used with a recommendation of genetic counseling and testing, which is frequently positive in such cases.³

One remarkable aspect of FH-deficient RCC is its aggressive behavior, with a high potential to metastasize early,⁶ mostly at the time of presentation.^{9,10} For this reason, these tumors initially may be sampled by fine-needle aspiration (FNA) or by core biopsy to establish a tissue diagnosis for treatment planning. The features of FH-deficient RCC in cytologic samples have not been characterized; therefore, to aid in the prospective recognition of this entity, we assembled and studied a cohort of cytologic samples from well characterized cases.

MATERIALS AND METHODS

This was a retrospective clinicopathologic, morphologic, and cytologic analysis of 21 cytology samples from 18 patients who had FH-deficient RCC confirmed by immunohistochemistry (FH-negative and/or 2SC-positive; N = 7; including 1 with an FH deletion identified in somatic tumor sequencing) or who had a germline *FH* mutation (N = 12). We also reviewed 3 small metastatic biopsy samples, including 2 from patients who had cytology preparations available, as listed in Table 1, and an additional metastasis biopsy sample (see Table 2, patient 8)^{10,14} for which there were no cytology preparations. Cases were identified by retrospective searches of pathology databases from 3 institutions with the approval of each institutional review board. The nephrectomy surgical pathology aspects of 5 of the FH-deficient RCCs have been described in detail in prior studies,^{9,10} an additional case was described as a case report¹⁴ without any review of associated cytologic or metastatic samples. Deidentified clinicopathologic data were collected through a review of patient medical records and surgical pathology reports. FH and 2SC immunostaining protocols have been previously reported.^{4,10} All cytologic slides were re-reviewed, and their features were tabulated by multiple genitourinary surgical pathologists (L.C., S.C.S., and A.J.G.) and cytopathologists (L.M., V.R., X.W., and O.L.).

RESULTS

Clinicopathologic Features of FH-Deficient RCCs

In total, 19 patients, including 6 women and 13 men (age range, 22–69 years; median age, 45 years) were identified. Twelve patients (63%) had germline *FH* mutations, whereas 7 had FH-deficient RCC based on FH-deficient immunophenotype and/or somatic sequencing. Stigmata associated with HLRCC syndrome included 5 patients with uterine leiomyomata (including 2 without germline mutation data) and 1 with cutaneous leiomyomata. Potential family history documented included a family history of RCC (N = 3), cutaneous leiomyoma (N = 1) and “skin rash” (N = 1). Table 2 summarizes the clinical findings for each patient.

Primary tumors ranged in size from 2.5 to 21.5 cm (median, 11.6 cm); 4 tumors were pathologically staged as pT4, 8 tumors were staged as pT3, 2 were staged as pT2, and 1 was staged as pT1. Three patients had advanced disease identified on imaging studies and did not undergo cytoreductive nephrectomy. The disease course was uniformly aggressive; 6 patients were dead of disease at <18 months (of which 5 had progressive, diffusely metastatic disease), and 6 were dead of disease between 18 and 64 months. All patients had lymph node or visceral metastatic disease at presentation. Figure 1 presents representative examples of imaging and histopathologic findings.

3.2 Findings in Cytologic Samples

In total, 21 cytologic samples corresponding to 18 patients were identified and reviewed retrospectively, sampling 7 malignant effusions (5 pleural, 2 ascites), 5 lymph nodes, 6 metastases (3 liver metastases and 1 each adrenal, chest wall, and pleural metastases), and 3 primary kidney tumors. Table 1 details the samples and the preparation types reviewed.

Cytologic preparations most frequently were cellular (n = 9) or moderately cellular (n = 7) rather than low in cellularity (n = 4), and the hypocellular samples corresponded to effusion samples in 3 of 4 preparations. All cases demonstrated striking, markedly enlarged, malignant cells with abundant, voluminous cytoplasm, nearly all of which presented at least focally in well defined, 3-dimensional clusters (20 of 21 cases; 95%) (Fig. 2A) or papillae (15 of 21 cases; 71%) (Fig. 2B,C)¹¹ in a background associated with chronic (13 of 21 cases; 62%) or mixed (2 of 21 cases; 10%) inflammation. The cytoplasm most frequently was finely vacuolated (18 of 21 cases; 86%) (Fig. 2D), as opposed to exhibiting variable large and small vacuoles (2 of 21 cases; 10%) or only large vacuoles (1 of 21 cases; 5%).

Findings that we deemed distinctive upon review were observed most prominently in Diff-Quik–stained preparations, including frequent peripheral clearing of cytoplasm, imparting a 2-toned appearance with paler cytoplasm toward the cell membrane (15 of 17 cases; 88%) (Fig. 3A,B). In addition, most prominent in Papanicolaou (Pap)-stained preparations (but less prevalent overall) were intranuclear cytoplasmic pseudoinclusions (6 of 21 cases; 29%) (Fig. 3C). Cytologic features that echoed those described in surgical pathology specimens for FH-deficient RCCs were prevalent, including enlarged, pleomorphic nuclei (21 of 21 cases; 100%) and prominent, inclusion-like macronucleoli (present in 21 of 21 cases [100%]; present only focally in 1 of 21 cases [5%]). The feature of perinucleolar halo-like clearing (Fig. 3D) was less prevalent (present in 10 of 21 cases [48%]; present only

focally in 4 of 21 cases [19%]) than inclusion-like macronucleoli. None of these cytologic parameters differed significantly between the cases designated as FH-deficient RCCs versus those associated with proven *FH* mutation.

3.3. Findings in Routine Sections From Biopsies and FNA Cell Blocks

In total, 11 samples processed for hematoxylin and eosin-stained sections were reviewed (10 from cytology samples and 1 additional metastasis core biopsy). These included FNA cell blocks (n = 3: kidney tumor, liver metastasis, and supraclavicular lymph node metastasis), core-needle biopsies (n = 6: kidney tumor, liver and adrenal metastasis), and small surgical biopsies (n = 2: lymph node metastasis and chest wall metastasis). The samples from primary renal tumors demonstrated various solid, tubular, papillary, and tubulocystic patterns in 2 cases (cores), and 1 fragment exhibited an intracystic papillary pattern with a hyalinized fibrovascular core in an FNA cell block from another case (Fig. 4A,B). The liver metastasis FNA cell block demonstrated scattered papillary fragments only, whereas 3 liver metastasis core biopsies exhibited tubulocystic, papillary, and focally cribriform patterns (Fig. 4C). An adrenal cortical metastasis core biopsy had a solid pattern. Two additional, small surgical biopsies were reviewed, including a supraclavicular lymph node resection, which had an extensive papillary pattern (Fig. 4D), and a chest wall metastasis, which had an infiltrative tubular and nested pattern. Intraoperative frozen sections from this chest wall lesion had been prepared and revealed features similar to those observed in permanent routine sections, albeit with less recognizable nucleolar features (Fig. 5).

4. DISCUSSION

FH-deficient RCCs, including those occurring in the syndromal setting of HLRCC, are aggressive tumors that frequently present with metastatic disease.⁶ For this reason, such tumors frequently may be sampled for initial diagnosis by aspiration cytology or core biopsy, or for confirmation of metastatic progression postresection. Although contemporary immunohistochemistry, including such markers as paired box gene 8 (PAX8), with correlation to imaging findings of a dominant renal mass, can help establish a renal primary origin,¹⁵ cytologic and rudimentary architectural features can provide important clues for the subclassification of RCC. Nonetheless, cytologic features of FH-deficient RCC have not been reviewed systematically, and, in our experience, these tumors remain under-recognized in both cytology and surgical pathology. Indeed, several of the older cases described herein originally had been designated as unclassified “type 2” papillary or were described as mixed RCC with clear and granular cell features. Given the emphasis on distinguishing between clear cell and nonclear cell RCC under current practice guidelines, the emerging clinical trial options for patients who have HLRCC syndrome, and the need for genetics consultation and surveillance among affected kindreds, we undertook the current retrospective review of the features of any cytologic and small biopsy samples taken during the diagnostic workup and management of these patients.

The overall findings in this cohort document that recognizable morphologic features related to those described for surgical pathology specimens of FH-deficient RCC may be observed in cytology specimens, and several additional, striking or distinctive cytologic features

also may be identified. In the case of the former, the presence of markedly enlarged and pleomorphic nuclei with striking, cytomegalovirus inclusion-like macronuclei were noted in every case, if variously prominent in any individual case. What was noted much less, and then only in Pap-stained preparations or in cell block material, was the characteristic (and more specific) feature of a perinucleolar halo of pallor in the nucleoplasm. Also reminiscent of histopathologic features was the formation of clusters, often cohesive with a 3-dimensional appearance, in direct smear samples.

However, 2 additional, distinctive cytologic features were identified. The first feature was voluminous, abundant cytoplasm in the neoplastic cells. Second, there was frequently a “2-toned” or variegated appearance, in which the most peripheral aspect of the cytoplasm, approaching the plasma membrane, demonstrated lighter staining or clearing compared with that observed in more central areas of Diff-Quik preparations. Characteristically (but not specifically), cytoplasmic vacuolation was apparent, usually as fine vacuolation with small vesicles. Less prevalent was the appearance of intranuclear cytoplasmic pseudoinclusions, reminiscent of papillary thyroid carcinoma, in Pap-stained slides from a subset of cases. Helpfully, when available, scant samples taken from metastases demonstrated architectural features that have been described as characteristic of⁸⁻¹⁰ and, in our recent comparative studies, distinctive for 19 FH-deficient RCCs, particularly with tubulocystic and intracystic papillary pattern, the latter with hyalinization of fibrovascular cores.

The differential diagnosis on cytologic grounds of a metastatic tumor in the setting of a suspected renal primary must focus on the most common and clinically actionable (under practice guidelines) entity in this differential, conventional clear cell RCC. Similar to findings from the FH-deficient tumors described herein, clear cell RCC cytology samples frequently have clustered cells with abundant cytoplasm (often finely vacuolated) and eccentric nuclei.¹⁶ Although they vary across World Health Organization/International Society of Urologic Pathology grades, nucleoli tend to be less prominent even in grade 3 and 4 conventional clear cell tumors compared with the remarkable, viral inclusion-like appearance in FH-deficient RCC samples. Whereas comprehensive studies of FH-deficient RCC immunophenotypes have not been performed, we emphasize that these tumors share positivity for PAX8 and, at least anecdotally, for CA-IX (carbonic anhydrase IX)^{3,17} with clear cell RCC, indicating the importance of correlations with any syndromal concerns and cytologic and morphologic features. We note that Xp11-translocation RCCs often exhibit abundant, voluminous cytoplasm in cytologic samples.¹⁸ Although decreased expression of pancytokeratins and melanocytic markers in translocation RCCs is characteristic and distinctive from FH-deficient RCCs (and other RCC types),^{18,19} these features are neither sufficiently sensitive nor specific to establish reliably the diagnosis of translocation RCC. Because the available antibodies against transcription factor E3 (TFE3) and transcription factor EB (TFEB) often are technically challenging, contemporary workup emphasizes the use of break-apart fluorescence in situ hybridization for the *TFE3* locus (or the *TFEB* locus for the less common t[6,11] translocation RCCs) as a definitive molecular test.²⁰

Given the frequent clustering and papillary architecture observed in most of our samples, the cytologic differential with conventional papillary RCC deserves mention. Although the presence of true fibrovascular cores may be shared, in no case of FH-deficient RCC

did we observe distention of cores with foamy macrophages, nor was the characteristic monomorphous appearance of conventional papillary RCC cytology^{16,21} or clear cell papillary RCC²² simulated by any FH-deficient RCC. Although we regard many such cases as unclassified RCCs with papillary architecture, the features of “type 2” papillary RCCs that have been described in aspiration cytologic samples²³ may be the closest simulant of FH-deficient RCC, containing large cells with prominent nucleoli. This latter finding emphasizes the importance of clinical correlation and the use of immunostains for triage, including FH and 2SC, which frequently are lost/reduced and strongly positive, respectively, in FH-deficient tumors. It also emphasizes consideration of emerging entities, such as a group of unclassified RCCs with *TFEB* amplification and melanocytic differentiation,^{20,24–26} which, in our experience, can strongly simulate the nucleolar features of FH-deficient RCCs.

The limitations of this cohort include its retrospective nature and the ascertainment and consultation biases of the referral institutions of the contributors. However, given the rarity of these tumors, such biases were necessary to assemble sufficient numbers for retrospective characterization. Challenging, too, remains the overall genetic interpretation of several cases of FH-deficient RCC retrieved from the files, for which data on neither syndromal stigmata nor genetic testing are available. Although we note that cases of FH-deficient RCC arising apparently by somatic mutation only have been identified,^{10,13} the degree of specificity of the FH-deficient phenotype for bona fide HLRCC syndrome with a germline *FH* mutation remains a principal unanswered question in the field. Increasingly, we argue that the recognition (whether based on cytologic, histomorphologic, or immunophenotypic features) of these tumors is a pathologist’s responsibility,¹ so that genetic counseling and testing may be undertaken. A recent study has documented relatively high rates of positive genetic testing for patients who were referred based on suspicious kidney tumor pathology.²⁷ Recent data also suggest that features like syndromal stigmata and family history should not be considered useful predictors of testing positive for RCC-predisposing syndromes (only young age had a significant association).²⁸

In summary, our current review of cytologic findings from cases of FH-deficient RCC has identified several features that, taken together, we believe will be sufficiently distinctive to enable the prospective recognition of these cases. Although much work remains to be done with regard to delineating the genetics of these tumors and discovering therapeutic angles, the recognition of these cases remains the first step.

Acknowledgments

FUNDING SUPPORT

No specific funding was disclosed.

Presented in part at the American Society of Clinical Pathology (ASCP) 2017 Annual Meeting; September 6-8, 2017; Chicago, Illinois; and at the 2018 United States and Canadian Academy of Pathology (USCAP) Annual Meeting; March 17-23, 2018; Vancouver, British Columbia, Canada

REFERENCES

1. Mochel MC, Smith SC. Kidney tumors associated with hereditary cancer syndromes: an emerging opportunity and responsibility in surgical pathology. *AJSP Rev Rep*. 2017;22:313–328.
2. Tomlinson IP, Alam NA, Rowan AJ, et al. Germline mutations in FH predispose to dominantly inherited uterine fibroids, skin leiomyomata and papillary renal cell cancer. *Nat Genet*. 2002;30:406–410. [PubMed: 11865300]
3. Muller M, Guillaud-Bataille M, Salleron J, et al. Pattern multiplicity and fumarate hydratase (FH)/S-(2-succino)-cysteine (2SC) staining but not eosinophilic nucleoli with perinucleolar halos differentiate hereditary leiomyomatosis and renal cell carcinoma-associated renal cell carcinomas from kidney tumors without FH gene alteration. *Mod Pathol*. 2018;31:974–983. [PubMed: 29410489]
4. Smith SC, Sirohi D, Ohe C, et al. A distinctive, low-grade onco-cytic fumarate hydratase-deficient renal cell carcinoma, morphologically reminiscent of succinate dehydrogenase-deficient renal cell carcinoma. *Histopathology*. 2017;71:42–52. [PubMed: 28165631]
5. Li Y, Reuter VE, Matoso A, Netto GJ, Epstein JI, Argani P. Reevaluation of 33 ‘unclassified’ eosinophilic renal cell carcinomas in young patients. *Histopathology*. 2018;72:588–600. [PubMed: 28898443]
6. Merino MJ, Torres-Cabala C, Pinto P, Linehan WM. The morphologic spectrum of kidney tumors in hereditary leiomyomatosis and renal cell carcinoma (HLRCC) syndrome. *Am J Surg Pathol*. 2007;31:1578–1585. [PubMed: 17895761]
7. Moch H, Humphrey PA, Ulbright TM, Reuter VE, eds. WHO Classification of Tumors of the Urinary System and Male Genital Organs. Volume 8. WHO Classification of Tumors. 4th ed. Lyon, France: IARC Press; 2016.
8. Trpkov K, Hes O, Agaimy A, et al. Fumarate hydratase-deficient renal cell carcinoma is strongly correlated with fumarate hydratase mutation and hereditary leiomyomatosis and renal cell carcinoma syndrome. *Am J Surg Pathol*. 2016;40:865–875. [PubMed: 26900816]
9. Chen YB, Brannon AR, Toubaji A, et al. Hereditary leiomyomatosis and renal cell carcinoma syndrome-associated renal cancer: recognition of the syndrome by pathologic features and the utility of detecting aberrant succination by immunohistochemistry. *Am J Surg Pathol*. 2014;38:627–637. [PubMed: 24441663]
10. Smith SC, Trpkov K, Chen YB, et al. Tubulocystic carcinoma of the kidney with poorly differentiated foci: a frequent morphologic pattern of fumarate hydratase-deficient renal cell carcinoma. *Am J Surg Pathol*. 2016;40:1457–1472. [PubMed: 27635946]
11. Ohe C, Smith SC, Sirohi D, et al. Reappraisal of morphologic differences between renal medullary carcinoma, collecting duct carcinoma, and fumarate hydratase-deficient renal cell carcinoma. *Am J Surg Pathol*. 2018;42:279–292. [PubMed: 29309300]
12. Carter CS, Skala SL, Chinnaiyan AM, et al. Immunohistochemical characterization of fumarate hydratase (FH) and succinate dehydrogenase (SDH) in cutaneous leiomyomas for detection of familial cancer syndromes. *Am J Surg Pathol*. 2017;41:801–809. [PubMed: 28288038]
13. Cancer Genome Atlas Research Network, Linehan WM, Spellman PT, et al. Comprehensive molecular characterization of papillary renal-cell carcinoma. *N Engl J Med*. 2016;374:135–145. [PubMed: 26536169]
14. Toon CW, Hasovits C, Paik J, et al. Skin rash, a kidney mass and a family mystery dating back to World War II. *Med J Aust*. 2014;201:58–60. [PubMed: 24999901]
15. Reuter VE, Argani P, Zhou M, Delahunt B; Members of the ISUP Immunohistochemistry in Diagnostic Urologic Pathology Group. Best practices recommendations in the application of immunohistochemistry in the kidney tumors: report from the International Society of Urologic Pathology consensus conference. *Am J Surg Pathol*. 2014;38:e35–e49. [PubMed: 25025368]
16. Lew M, Foo WC, Roh MH. Diagnosis of metastatic renal cell carcinoma on fine-needle aspiration cytology. *Arch Pathol Lab Med*. 2014;138:1278–1285. [PubMed: 25268189]
17. Udager AM, Alva A, Chen YB, et al. Hereditary leiomyomatosis and renal cell carcinoma (HLRCC): a rapid autopsy report of metastatic renal cell carcinoma. *Am J Surg Pathol*. 2014;38:567–577. [PubMed: 24625422]

18. Schinstine M, Filie AC, Torres-Cabala C, Abati A, Linehan WM, Merino M. Fine-needle aspiration of an Xp11.2 translocation/TFE3 fusion renal cell carcinoma metastatic to the lung: report of a case and review of the literature. *Diagn Cytopathol.* 2006;34:751–756. [PubMed: 17121198]
19. El Naili R, Nicolas M, Gorena A, Policarpio-Nicolas ML. Fineneedle aspiration findings of Xp11 translocation renal cell carcinoma metastatic to a hilar lymph node. *Diagn Cytopathol.* 2017;45:456–462. [PubMed: 28185421]
20. Skala SL, Xiao H, Udager AM, et al. Detection of 6 TFE3-amplified renal cell carcinomas and 25 renal cell carcinomas with MITF translocations: systematic morphologic analysis of 85 cases evaluated by clinical TFE3 and TFE3 FISH assays. *Mod Pathol.* 2018;31:179–197. [PubMed: 28840857]
21. Granter SR, Perez-Atayde AR, Renshaw AA. Cytologic analysis of papillary renal cell carcinoma. *Cancer.* 1998;84:303–308. [PubMed: 9801205]
22. Sayeed S, Lindsey KG, Baras AS, et al. Cytopathologic features of clear cell papillary renal cell carcinoma: a recently described variant to be considered in the differential diagnosis of clear cell renal epithelial neoplasms. *Cancer Cytopathol.* 2016;124:565–572. [PubMed: 27062008]
23. Renshaw AA, Cibas ES. Kidney and adrenal gland. In: Cibas ES, Ducatman BS, eds. *Cytology. Diagnostic Principals and Clinical Correlates.* 4th ed. New York: Elsevier; 2014:423–451.
24. Gupta S, Johnson SH, Vasmataz G, et al. TFE3-VEGFA (6p21.1) co-amplified renal cell carcinoma: a distinct entity with potential implications for clinical management. *Mod Pathol.* 2017;30:998–1012. [PubMed: 28338654]
25. Martin EE, Mehra R, Jackson-Cook C, Smith SC. Renal cell carcinoma with TFE3 translocation versus unclassified renal cell carcinoma with TFE3 amplification. *AJSP Rev Rep.* 2017;22:305–312.
26. Williamson SR, Grignon DJ, Cheng L, et al. Renal cell carcinoma with chromosome 6p amplification including the TFE3 gene: a novel mechanism of tumor pathogenesis? *Am J Surg Pathol.* 2017;41:287–298. [PubMed: 28009604]
27. Kopp RP, Stratton KL, Glogowski E, et al. Utility of prospective pathologic evaluation to inform clinical genetic testing for hereditary leiomyomatosis and renal cell carcinoma. *Cancer.* 2017;123:2452–2458. [PubMed: 28171700]
28. Stratton KL, Alanee S, Glogowski EA, et al. Outcome of genetic evaluation of patients with kidney cancer referred for suspected hereditary cancer syndromes [serial online]. *Urol Oncol.* 2016;34:238.e1-e7.

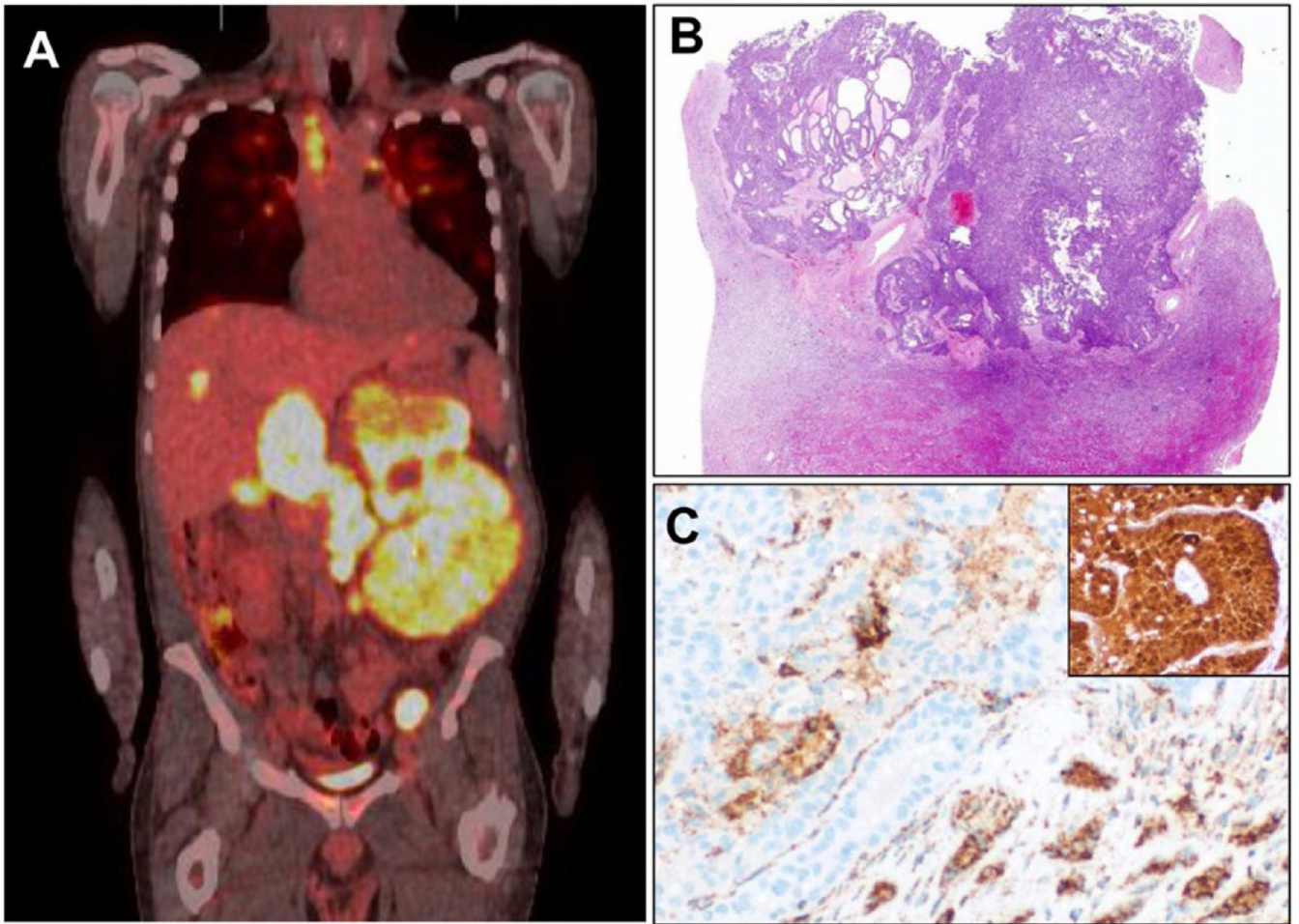


Figure 1.

Photomicrographs depict clinical findings in fumarate hydratase (FH)-deficient renal cell carcinoma (RCC). (A) A representative positron emission tomography scan exhibited uptake corresponding to an unresectable, left-sided kidney tumor; extensive retroperitoneal, pelvic, and mediastinal lymphadenopathy; and liver metastasis (patient 4). (B) A representative FH-deficient RCC had a solid and tubulocystic appearance (patient 2) at low power. (C) Identified only retrospectively, this case exhibited the complete loss of FH on immunohistochemistry, (*inset*) with diffuse nucleocytoplasmic staining for antibodies that detect anti-S-(2-succino)-cystine (2SC), documenting the FH-deficient immunophenotype. No sequencing tests were available, although the patient had uterine leiomyomatosis described as extensive on staging radiography.

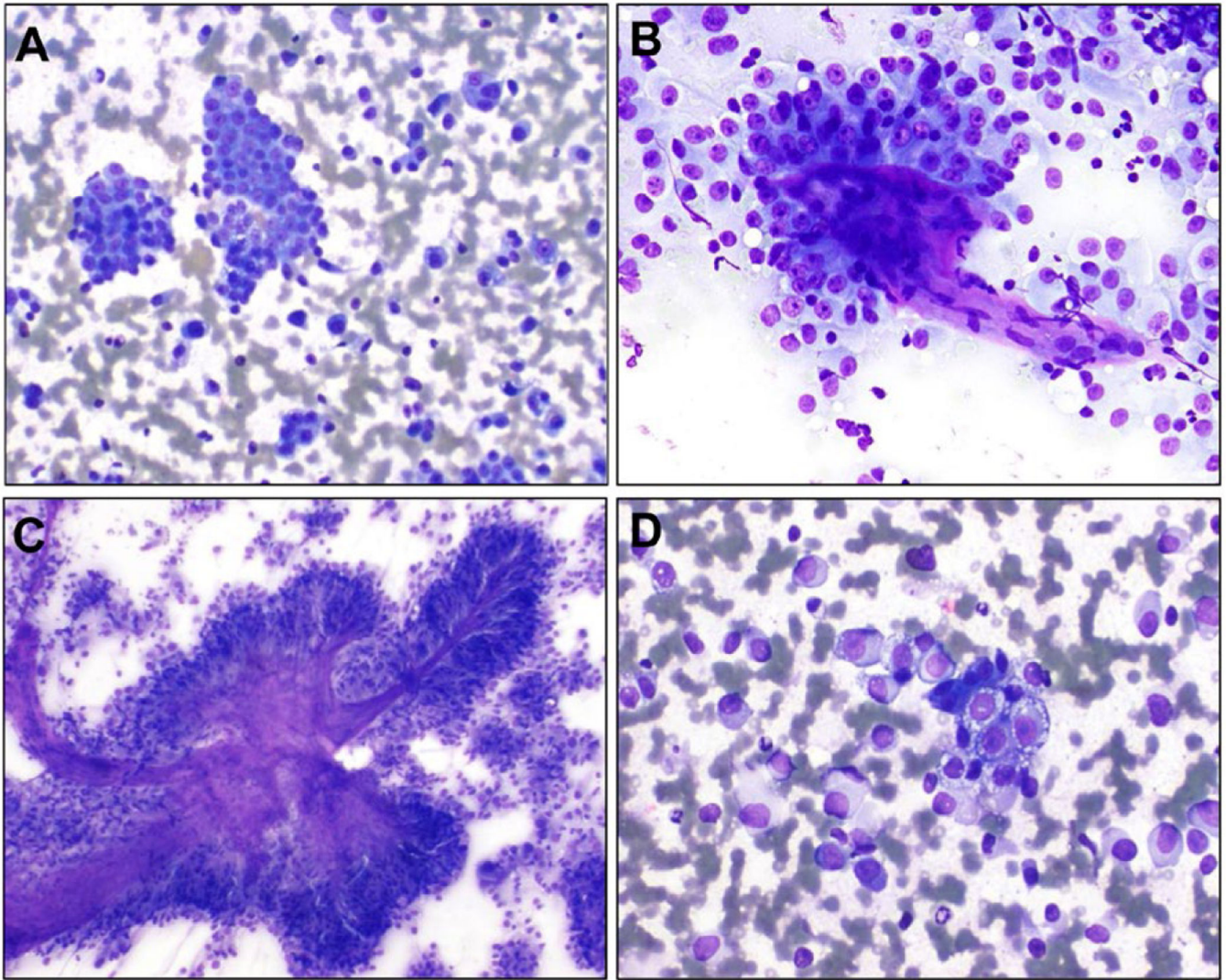


Figure 2.

Photomicrographs reveal prevalent findings in cytologic samples of fumarate hydratase-deficient renal cell carcinomas. (A) Most cytologic samples were relatively cellular, with well formed, 3-dimensional clusters identified in nearly all cases. (B) In many cases, some of the clusters exhibited the formation of abortive papillae, with occasional associated fibrovascular cores. (C) In a subset of cases (particularly touch preparations from core biopsy samples), exaggerated, large papillary structures with copious, metachromatic stroma were apparent and were deemed to represent papillae with hyalinized cores, a feature strongly associated with fumarate hydratase-deficient renal cell carcinoma in surgical specimens.¹⁰ (D) At higher power magnification, the sampled cells exhibited significant pleomorphism, often with eccentric nuclei, and prominent nuclei were apparent in Diff-Quik stains. Frequently, the cytoplasm had fine vacuolation.

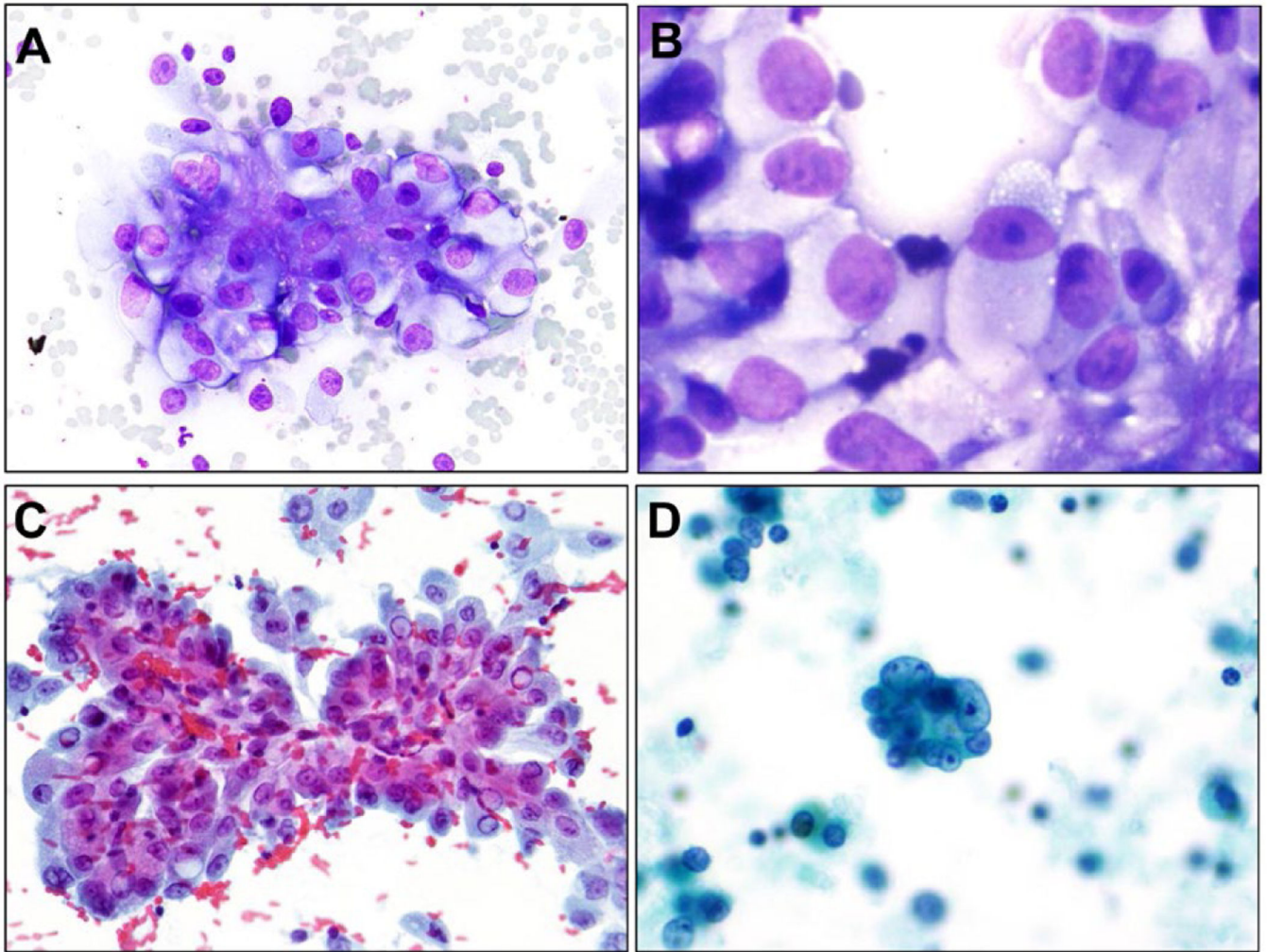


Figure 3.

Photomicrographs reveal distinctive findings in cytologic samples of fumarate hydratase (FH)-deficient renal cell carcinomas (RCCs). (A) One frequent cytologic finding that was deemed striking with regard to FH-deficient RCC was the appearance of a 2-toned or variegated appearance of the cytoplasm, in which the peripheral aspects of the cytoplasm appeared lighter or clearer than in more central areas. (B) At higher power, the center FH-deficient RCC cell demonstrates a striking macronucleolus, which is a common feature in cytologic samples. At the periphery of the cell, small vacuoles are present, as is the aforementioned peripheral cytoplasmic clearing. (C) One less frequent but distinctive feature observed in this Papanicolaou-stained sample was intranuclear cytoplasmic pseudoinclusions. (D) The reported hallmark of FH-deficient RCC (a halo-like, perinucleolar clearing around the inclusion-like macronucleolus) was not frequently apparent in cytologic samples. In some Papanicolaou-stained and cell block preparations, a suggestion of perinucleolar clearing was apparent.

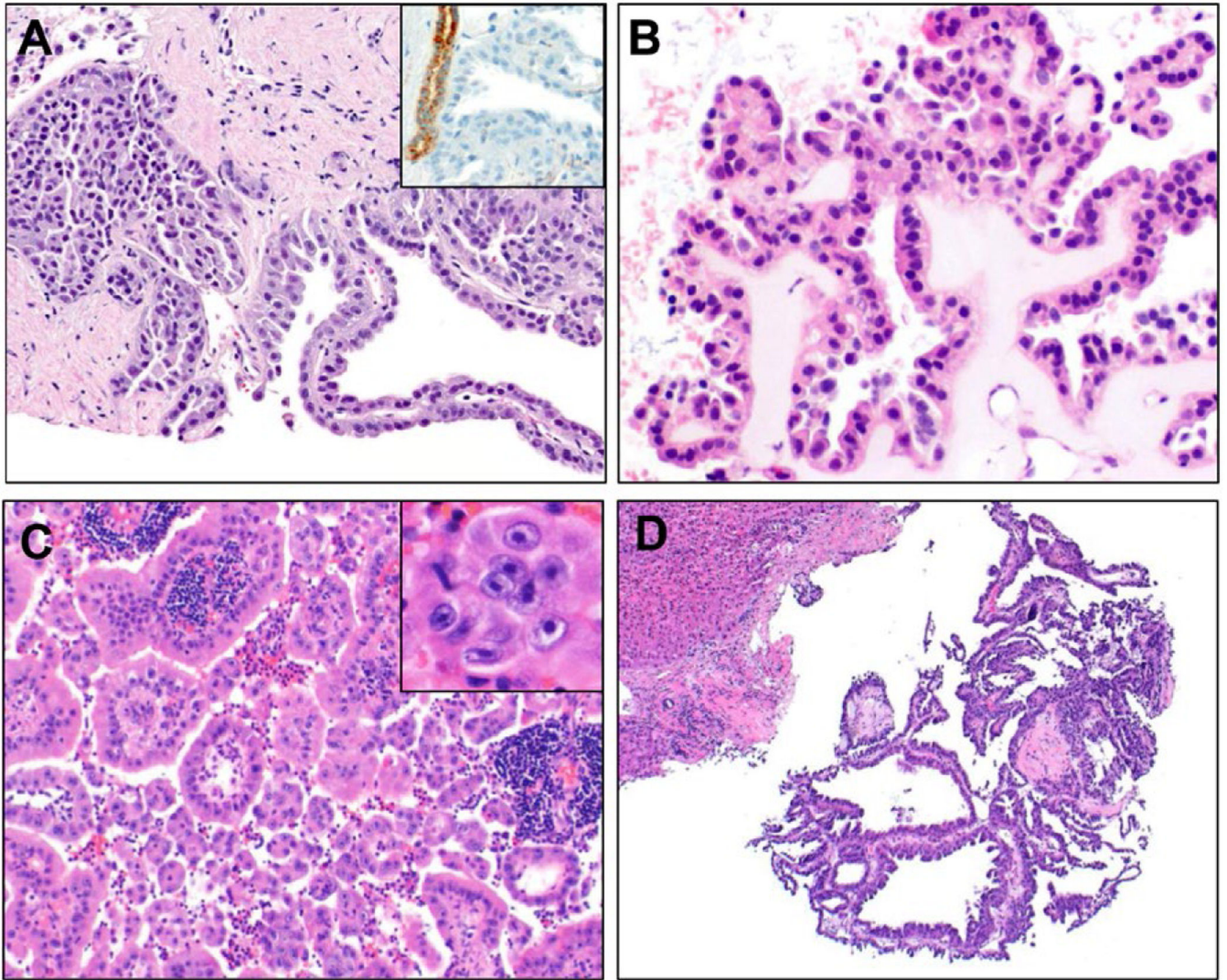


Figure 4.

Primary and metastatic, fumarate hydratase-deficient renal cell carcinomas are shown on photomicrographs of routine H&E-stained sections. (A) This representative intermediate power magnification of a kidney core biopsy (patient 4) exhibited a variable solid and tubulocystic pattern. (*Inset*) Immunohistochemistry revealed that the tumor had complete loss of fumarate hydratase, with preserved, internal control-entrapped tubules (left on *inset*). (B) A fine-needle aspiration cell block sample from another primary renal tumor (patient 2) had a fragment with an intracystic papillary pattern and hyalinized cores. (C) A supraclavicular lymph node biopsy (patient 3) exhibited a confluent papillary pattern with (*inset*) prominent, inclusion-like nucleoli and perinucleolar halos. (D) Core biopsy of a liver metastasis (patient 8) revealed a tubulocystic pattern.

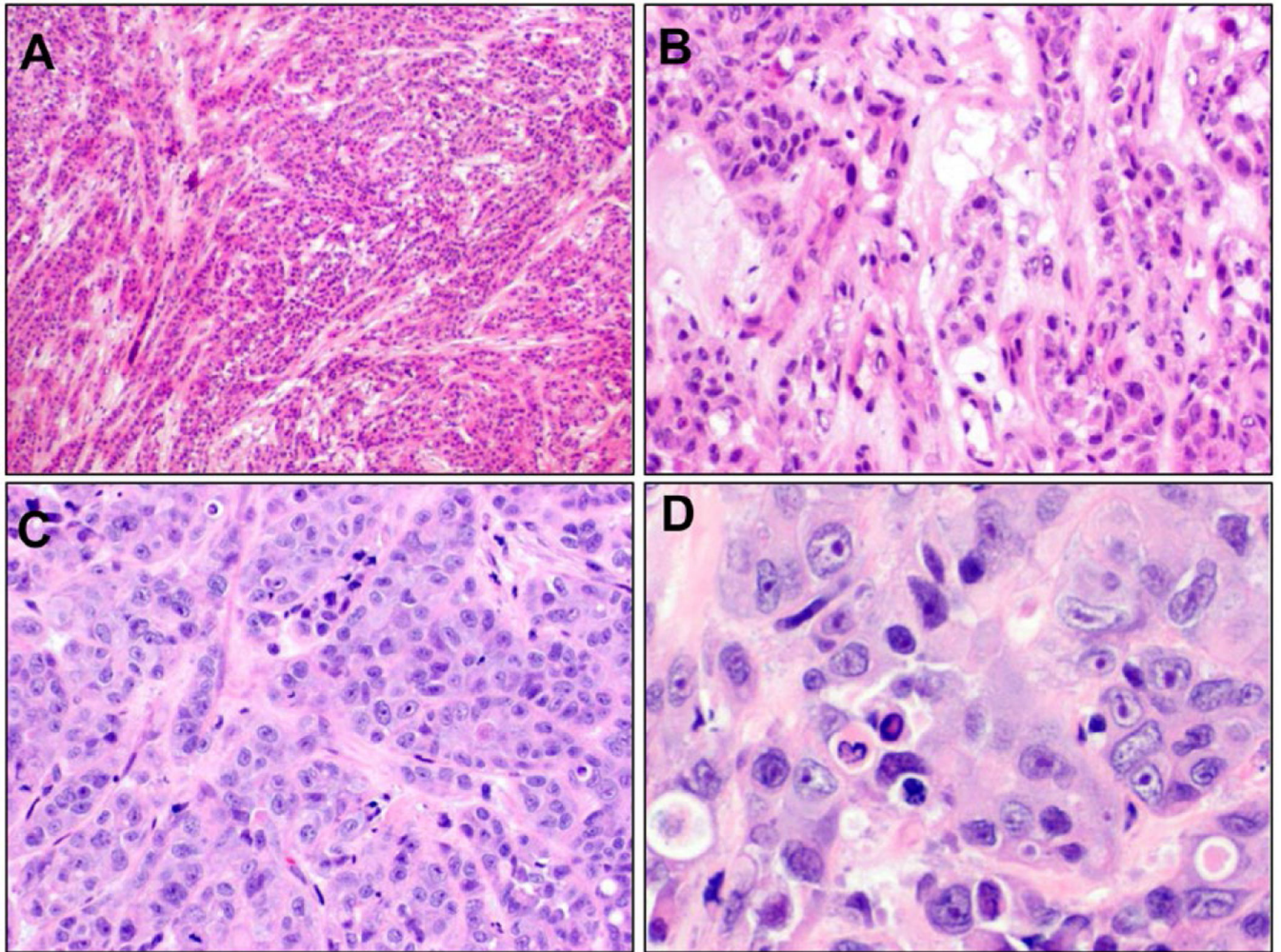


Figure 5. Photomicrographs reveal frozen-section findings from a metastatic biopsy of fumarate hydratase-deficient renal cell carcinoma. (A) At lower power, frozen sections of a chest wall metastasis revealed an infiltrative, adenocarcinomatous pattern. (B) Higher power magnification revealed plump, epithelioid cells in a tubular and nested, adenocarcinomatous pattern with large, pleomorphic nuclei. Nucleolar features were not present. (C) Permanent sections from this case exhibited the classic appearance of fumarate hydratase-deficient renal cell carcinoma, including a high-grade, syncytial pattern with (D) large, pleomorphic nuclei and classic nuclear features.

TABLE 1.

Cytology Samples Reviewed and Features Observed

Sample No.	Patient No.	Sample Site	Preparations	Cellularity	3D Clusters	Papillae	Inflammation	Prominent Nucleoli	Abundant Cybotomiasm	Cybotomiasmic Clearing ^d	Perinuclear Halos	Vaculation	INPI
1	1	PF	DQ (CS), Pap (CS), CB	Moderate	Yes	No	Chronic	Yes	Yes	Yes	Rare	Large	No
2	1	CW mets	DQ (TP) ^b	High	Yes	Yes	None	Yes	Yes	Yes	No	Large and small	Yes
3	2	LV mets	DQ (SM), Pap (SM), CB	High	Yes	Yes	None	Yes	Yes	Yes	Present	Large and small	No
4	2	KD	DQ (SM), CB	Scant	Yes	Yes	Chronic	Yes	Yes	Yes	No	Small	Rare
5	3	LN	DQ (SM), Pap (SM), CB	High	Yes	Yes	Chronic	Yes	Yes	No	Diffuse	Small	Yes
6	4	KD	DQ (TP), core	Moderate	Yes	Yes	Chronic	Yes	Yes	Yes	Rare	Small	Rare
7	5	PF	Pap (SM)	Moderate	Yes	Yes	Chronic	Yes	Yes	NA ^c	Rare	Small	No
8	5	PNF	Pap (SM)	Moderate	Yes	Yes	Chronic	Yes	Yes	NA ^c	No	Small	No
9	6	PCM	DQ (SM), Pap (SM), CB	High	Yes	Yes	None	Yes	Yes	Yes	Rare	Small	Rare
10	7	AF	DQ (SM), Pap (SM), CB	Scant	Yes	Yes	Mixed	Yes	Yes	No	Present	Small	No
11	9	PF	DQ (SM), Pap (SM), CB	Low	Yes	Yes	Chronic	Yes	Yes	Yes	No	Small	No
12	10	LV mets	DQ (TP), Pap (TP), core	High	Yes	No	None	Yes	Yes	Yes	Present	Small	No
13	11	RP LN	DQ (TP), Pap (TP), core	High	Yes	Yes	None	Yes	Yes	Yes	No	Small	No
14	12	LN	DQ (SM), Pap (SM), CB	High	Yes	Yes	Chronic	Yes	Yes	Yes	Present	Small	No
15	13	LV mets	DQ (TP), Pap (TP), core	High	Yes	Yes	Chronic	Yes	Yes	Yes	No	Small	No
16	14	A	DQ (TP), Pap (TP), core	Moderate	Yes	No	Chronic	Yes	Yes	Yes	No	Small	No
17	15	LN	DQ (SM), Pap (SM), CB	High	Yes	Yes	Chronic	Yes	Yes	Yes	Present	Small	Yes
18	16	LN	DQ (SM), Pap (SM), CB	Moderate	Yes	No	Chronic	Yes	Yes	Yes	No	Small	No

Sample No.	Patient No.	Sample Site	Preparations	Cellularity	3D Clusters	Papillae	Inflammation	Prominent Nucleoli	Abundant Cybotomlasm	Cybotomlasmic Clearing ^a	Perinucleolar Halos	Vacuolation	INPI
19	17	PF	Pap (SM), CB	Moderate	Yes	No	Mixed	Yes	Yes	NA ^c	No	Small	No
20	18	PF	Pap (SM), CB	Low	No	No	Chronic	Yes	Yes	NA ^c	No	Small	No
21	19	KD	DQ (TP), Pap (TP), core	Moderate	Yes	Yes	None	Yes	Yes	Yes	No	Small	No

Abbreviations: 3D, 3-dimensional; A, adrenal; AF, ascitic fluid; CB, cell block; CS, cytospin; CW, chest-wall; DQ, Diff-Quik; INPI, intranuclear pseudo-inclusions; KD, kidney; LN, lymph node; LV, liver; mets, metastasis; Pap, Papanicolaou stain; PCM, pleural cavity mass; PF, pleural fluid; PNF, peritoneal fluid; RP LN, retroperitoneal lymph node; SM, smear preparation; TP, touch preparation.

^aCytoplasmic clearing was evaluated on DQ preparations.

^bThis preparation was performed on a surgical specimen.

^cNA indicates that data were not available for specimens that did not include a DQ preparation.

TABLE 2.

Clinicopathologic Features

Patient No.	FH Status Findings	HLRCC Stigmata	Sex	Age, y	Laterality	Tumor Size, cm	Stage	LN Metastasis	Metastasis	Outcome	Follow-Up, mo
1	FH-2SC+, FH deletion (Smith 2016 ¹⁰)	UL	W	42	Left	4.1	pT3a	No	LG, E, CW	DOD	3
2	FH-2SC+	UL	W	35	Right	10.0	pT2	No	LG, LV	DOD	13
3	FH-	None	M	69	Right	Unknown	cT4 (unresected)	RP LN	LV, OM, BN	DOD	14
4	FH-	None	M	53	Left	11.6	cT3b (unresected)	RP LN	A, LV, BN, LG	AWD	20
5	FH-/2SC+ (Smith 2016 ¹⁰)	Unknown	M	35	Left	13.6	pT3	RP LN	A, BN, E	DOD	9
6	FH-/2SC+ (Smith 2016 ¹⁰)	Unknown	M	51	Right	21.5	pT2b	No	LG	DOD	10
7	Germline FH mutation (Toon 2014 ¹⁴)	CL; Fam rash and RCC	M	25	Right	14.0	pT3a	RP LN	LV, CW	DOD	64
8 ^a	FH-	Unknown	M	51	Left	21.6	NA	NA	LV - core reviewed	AWD	6
9	Germline FH mutation	UL	W	60	Right	2.5	pT1	RP LN	PL, BN, LV, SP	DOD	144
10	Germline FH mutation	UL	W	43	Left	6.8	pT3	RP LN	LV, LG	DOD	46
11	Germline FH mutation	Fam CL	M	54	Left	6.0	pT4	RP LN	LV, A	DOD	22
12	Germline FH mutation	Fam RCC	M	44	Left	4.6	pT3	RP LN	LN	DOD	34
13	Germline FH mutation	None	M	53	Right	8.0	pT3	RP LN	LN, LV, A, LG	AWD	41
14	Germline FH mutation	UL	W	54	Left	7.0	pT4	RP LN	LG, A	DOD	23
15	Germline FH mutation	None	M	61	Left	1.5	pT4	RP LN	LN, A, PL, BN, LV	DOD	8
16	Germline FH mutation	None	M	42	Left	6.5	pT3	RP LN	A	AWD	15
17	Germline FH mutation	None	W	22	Left	9.2	pT4	No	LG, BN, OV	DOD	31
18	Germline FH mutation	Fam RCC	M	45	Left	13.6	pT3	RP LN	A, PL, LV, LN	AWD	2.5
19	Germline FH mutation	None	M	24	Right	8.6	NA	RP LN	BN, LG, LN	AWD	12

Abbreviations: -, negative; +, positive; A, adrenal; AWD, alive with disease; BN, bone; CL, cutaneous leiomyomata; cT, clinical tumor classification; CW, chest wall; DOD, died of disease; E, effusion; Fam, family history of indicated feature; FH, fumarate hydratase; FH, fumarate hydratase gene; HLRCC, hereditary leiomyomatosis-renal cell carcinoma syndrome; LG, lung; LN, lymph node; LTFU, lost to follow-up; LV, liver; M, man; NA, not available; OM, omentum; OV, ovary; PL, pleura; RCC, renal cell carcinoma; pT, pathologic tumor classification; RP LN, retroperitoneal lymph node; 2SC, S-(2-succino)-cysteine; SP, spleen; UL, uterine leiomyomata; Unk, unknown; W, woman.

^aThis patient underwent core biopsy only, without a touch or other cytologic preparation, and thus is not listed in Table 1.